LETTERS
https://doi.org/10.1038/s41558-019-0677-4

nature climate change

Addendum

Substantial twentieth-century Arctic warming caused by ozone-depleting substances

L. M. Polvani[1,2*], M. Previdi[2], M. R. England[1], G. Chiodo[1,3] and K. L. Smith[2,4]

The rapid warming of the Arctic, perhaps the most striking evidence of climate change, is believed to have arisen from increases in atmospheric concentrations of GHGs[1] since the Industrial Revolution. While the dominant role of carbon dioxide is undisputed, another important set of anthropogenic GHGs was also being emitted over the second half of the twentieth century: ozone-depleting[2] substances (ODS). These compounds, in addition to causing the ozone hole over Antarctica, have long been recognized[3] as powerful GHGs. However, their contribution to Arctic warming has not been quantified. We do so here by analysing ensembles of climate model integrations specifically designed for this purpose, spanning the period 1955–2005 when atmospheric concentrations of ODS increased rapidly. We show that, when ODS are kept fixed, forced Arctic surface warming and forced sea-ice loss are only half as large as when ODS are allowed to increase. We also demonstrate that the large impact of ODS on the Arctic occurs primarily via direct radiative warming, not via ozone depletion. Our findings reveal a substantial contribution of ODS to recent Arctic warming, and highlight the importance of the Montreal Protocol as a major climate change-mitigation treaty.

Ozone-depleting substances (ODS, see Methods), organic halogen compounds with long atmospheric lifetimes (for example, chlorofluorocarbons), were developed in the 1920s and 1930s for use as refrigerants, solvents and propellants, and started being emitted in substantial quantities into the atmosphere in the late 1950s. It is now well established[4] that these anthropogenic substances have been the primary cause of stratospheric ozone depletion. The discovery of the ozone hole[5] over Antarctica led to the phase-out of their production with the signing of the Montreal Protocol in 1987. As a consequence, the concentrations of most ODS peaked in the late twentieth century and have been declining[6] since then. In the intervening half-century, however, ODS have had a profound impact on the climate system.

Most research to date has focused on the climate impacts of ODS via changes in stratospheric ozone. Ozone depletion has not resulted in detectable surface-temperature changes, since its radiative forcing is very small[7] (<0.1 W m^{-2} in the global mean). However, polar lower stratospheric cooling accompanying the ozone hole is very large[8] (>10 °C over the period 1969–1998) and has caused changes in the tropospheric circulation[9,10], with many associated climate impacts[11,12] reaching from the South Pole to the tropics, although confined to the Southern Hemisphere.

Little research, in contrast, has focused on the climate impacts of ODS that are independent of ozone depletion. While much less abundant than carbon dioxide, ODS are much more powerful[13–15] GHGs on a molecule-by-molecule basis. For instance, chlorofluorocarbons CFC-11 and CFC-12 are 19,000- and 23,000-fold[7] more radiatively efficient, respectively, than CO_2 (in terms of W m^{-2} per parts per billion), resulting in 20-year global warming potentials 7,000- and 11,000-fold larger[6], respectively, than CO_2, with similarly large numbers for most other ODS. As a consequence, the radiative forcing (RF) associated with ODS is considerable. While it is customary to compute RF from the pre-industrial era to the present, in this paper we focus specifically on the period 1955–2005, during which ODS concentrations grew rapidly. Over that period the RF from ODS is estimated[16] to be 0.31 W m^{-2}, which amounts to nearly one-third of the RF from CO_2 (1.02 W m^{-2}), making ODS, collectively, the second most important GHG in the latter half of the twentieth century, as seen in Fig. 1. These facts are well established[7,17] and the important contribution of ODS to global warming has previously been noted[18,19]. Beyond that, however, the climatic consequences of the large RF from ODS remain largely unexplored, notably over the Arctic.

Arctic surface temperatures have been rising at over twice the global mean rate[20], accompanied by a dramatic reduction in sea-ice extent (SIE) and thickness[21]. Because ODS have provided a substantial fraction (24%) of global total anthropogenic RF over the second half of the twentieth century[16], one is led to ask whether some substantial fraction of Arctic climate change might be attributable to increased ODS concentrations over that period. This is the key question we seek to answer.

We accomplish this by contrasting two ten-member ensembles of integrations with the CAM5LE climate model (see Methods) over the period 1955–2005. The first ten-member ensemble—denoted Historical—consists of the first ten members of the historical integrations performed by the Large Ensemble Project[22]: these integrations are forced with all known natural and anthropogenic forcings, and are intended to simulate the complete climate evolution. The second ten-member ensemble—denoted FixODSO3—is forced identically, except for ODS (which are kept fixed at 1955 levels) and stratospheric ozone (also kept fixed at 1955 levels, to be physically consistent). All members of each ensemble are forced identically, and differ only in their atmospheric initial condition: averaging over each ensemble reveals the forced response, with little contamination from internal variability[23].

Consider first the impact of ODS on the global mean surface air temperature (T_s). In our CAM5LE integrations, over the half-century 1955–2005 annual mean T_s increased by 0.59 °C in the Historical ensemble, but by only 0.39 °C in the FixODSO3 ensemble. In the absence of increasing ODS, therefore, global warming would have been one third smaller over that period. This result is very robust and holds true for every month of the year (see Extended Data Fig. 1a).

[1]Department of Applied Physics and Applied Mathematics, Columbia University, New York, NY, USA. [2]Lamont Doherty Earth Observatory, Columbia University, Palisades, NY, USA. [3]Institute for Atmospheric and Climate Sciences, ETH, Zurich, Zurich, Switzerland. [4]Department of Physical and Environmental Sciences, University of Toronto Scarborough, Toronto, Ontario, Canada. *e-mail: lmp@columbia.edu

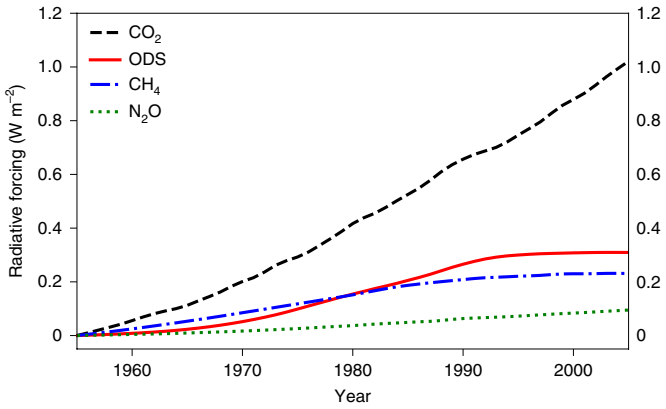

Fig. 1 | Radiative forcing of GHGs for 1955–2005. Global radiative forcing of the four principal well-mixed GHG from 1955 to 2005, as computed[16] from the data available at http://www.pik-potsdam.de/~mmalte/rcps.

Next, let us focus on the Arctic: again, annual mean T_s trends in that region are considerably stronger in the Historical than in the FixODSO3 ensemble, as seen by contrasting Fig. 2a and Fig. 2b. Specifically, our model shows a polar cap (60–90° N) average annual mean warming from 1955 to 2005 of 1.59 °C for the Historical ensemble, but of only 0.82 °C in the FixODSO3 ensemble (see Extended Data Fig. 1b for seasonal variations). In CAM5LE, therefore, ODS contributed almost 0.8 °C to forced Arctic surface warming in the latter half of the twentieth century.

A similar result applies to the loss of sea ice. In September, the month with the largest trends, sea-ice loss is greatly enhanced by increasing ODS concentrations, as seen by contrasting Fig. 2d and Fig. 2e. In that month, total SIE from 1955 to 2005 decreased by only 0.76×10^6 km^2 in the FixODSO3 ensemble, but by 1.45×10^6 km^2 in the Historical ensemble, a factor of almost two (with similar factors in other months of the year; Extended Data Fig. 1c). In CAM5LE, therefore, ODS contributed nearly 0.7×10^6 km^2 to the forced September Arctic sea-ice loss in the latter half of the twentieth century.

These results are summarized in Fig. 3, where the entire distribution of changes for each ensemble is shown for global and Arctic annual mean T_s, and for September SIE. First, note that the observed value of the 1955–2005 changes, denoted by the red dots, falls within the distribution of the ten Historical integrations for each of the three quantities (global T_s, Arctic T_s and SIE). This indicates that our model is able to capture the observations. Second, note that while internal variability can be substantial (as seen in the spread across each ten-member ensemble), in each panel of Fig. 3 the mean changes for the Historical and FixODSO3 ensembles are significantly different from each other at the 99.9% confidence level (by two-tailed t-test). This is perhaps not surprising, given that ODS contribute a substantial fraction of the change in Arctic T_s and September SIE for the period 1955–2005. We

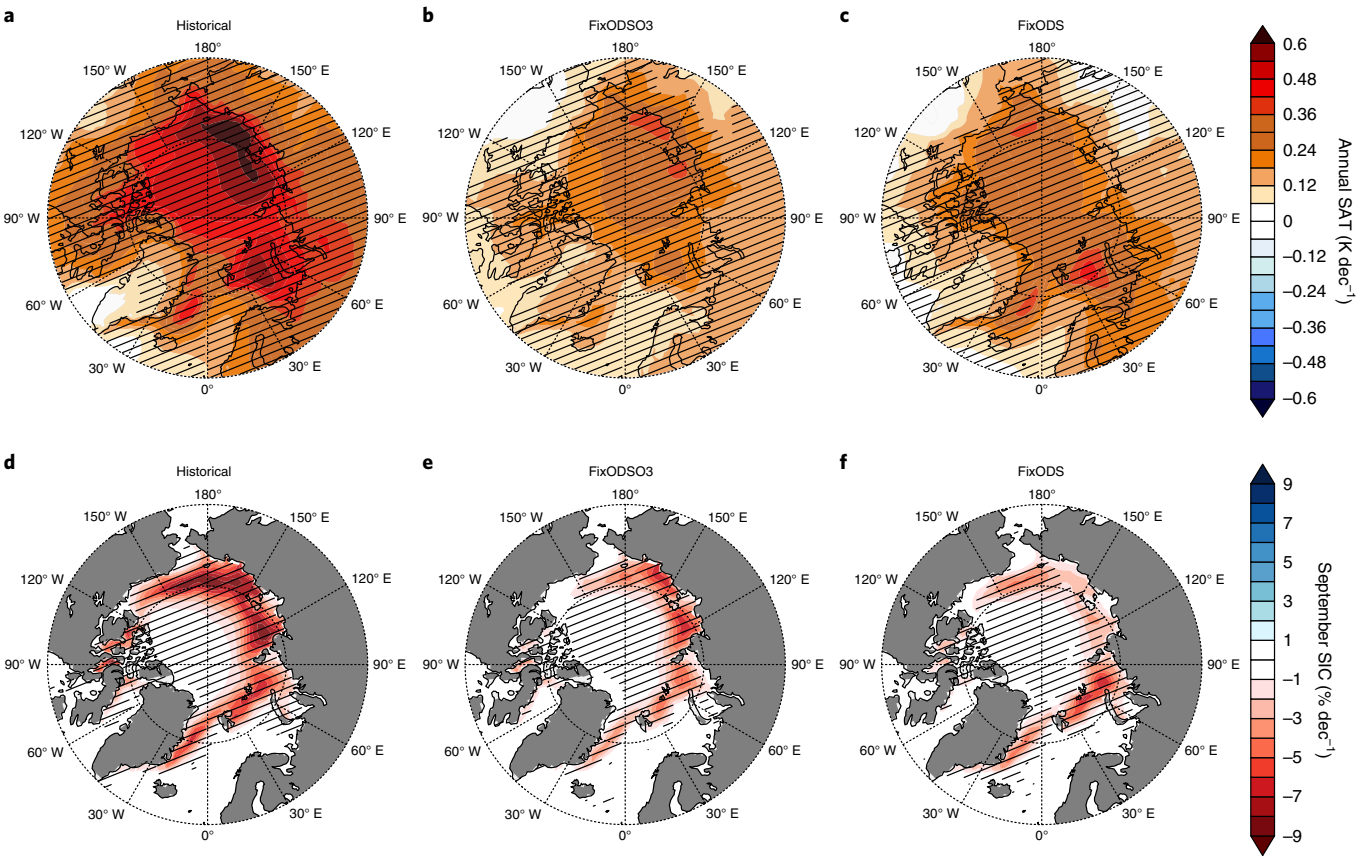

Fig. 2 | Arctic surface-temperature and sea-ice trends for 1955–2005. a–c, Ensemble mean surface air temperature (SAT, T_s) trends over the period 1955–2005 for the Historical (**a**), FixODSO3 (**b**) and FixODS (**c**) ensembles as computed by the CAM5LE model. **d–f**, As in **a–c**, but for sea-ice concentration (SIC). Statistically significant trends at the 95% level, as determined by two-sided t-test, are indicated by hashing. Trends in the Historical ensemble illustrate the forced response in the presence of all natural and anthropogenic forcings; trends in the FixODSO3 ensemble illustrate the response when both ODS and ozone are unchanged (except for seasonal variations) and remain constant at 1955 values; trends in the FixODS ensemble illustrate the response when only ODS are held fixed at 1955 values.

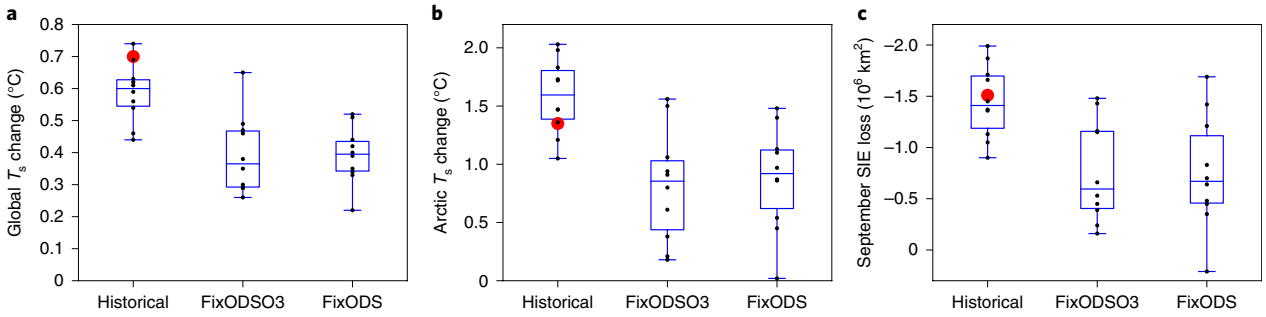

Fig. 3 | Climate impact of ODS for 1955–2005. a, Annual mean global surface-temperature change over the period 1955–2005 for each ten-member CAM5LE ensemble, as labelled on the abscissa. The boxes extend from the lower to upper quartile of the data, with a line at the median and whiskers showing the entire range across each ensemble; individual members are denoted by small black dots. **b**, As in **a** for Arctic temperatures, averaged (60–90° N). **c**, As in **a** but for September SIE. Red dots denote the observed values obtained from GISTEMP[27] v.3 for surface temperature and HadISST[28] v.2.2.0 for sea ice. In each panel, the means of the FixODSO3 and FixODS ensembles are significantly different from that of the Historical ensemble at the 99% confidence level by two-tailed *t*-test.

also note that ODS contribute to Arctic amplification over that period (see Extended Data Fig. 2): in CAM5LE, the Arctic polar cap warmed 2.7-fold more than the global mean in the Historical ensemble, but only twofold more without the contribution of ODS in the FixODSO3 ensemble.

Given the large internal variability of the Arctic climate system, one may wonder whether ensembles of ten simulations are sufficient to establish a robust difference between the Historical and FixODSO3 simulations. Going beyond a simple *t*-test and without performing additional model integrations, we address this question using a standard bootstrapping technique (resampling with replacement) to create 10,000-member synthetic probability distributions (PDFs) of 1955–2005 changes from the original ten-member ensembles. For each of the three variables in Fig. 3, the PDFs for Historical and FixODSO3 changes are shown in Extended Data Fig. 3: the almost total separation of the two PDFs confirms that ten integrations are more than sufficient to establish the large impact of ODS on Arctic climate over the period of interest.

We now ask whether these large impacts of ODS on climate are directly linked to their being potent GHGs, or indirectly mediated by the depletion of stratospheric ozone. To answer that question we analysed an additional ten-member ensemble—denoted FixODS—where only the atmospheric concentrations of ODS are fixed at 1955 levels while stratospheric ozone is allowed to vary as in the Historical CAM5LE ensemble (Fig. 2c,f). There are no statistically significant differences, annually or monthly, between the FixODS and FixODSO3 ensembles for T_s and SIE (Fig. 3 and Extended Data Fig. 1). We conclude, therefore, that the direct radiative forcing of ODS, not stratospheric ozone depletion, is the primary mechanism.

It is also legitimate to ask whether such a large contribution of ODS to Arctic warming might be an artefact of the CAM5LE model. To answer that question, we carried out an almost identical exercise—two ensembles of runs, with and without ODS and ozone changes—with the Whole Atmosphere Community Climate Model (WACCM4, see Methods). Unlike CAM5LE, WACCM4 includes interactive chemistry for stratospheric ozone, which is then consistent with the circulation. The WACCM4 results corroborate the CAM5LE findings (see Extended Data Fig. 4). In WACCM4 too, the Arctic impacts of ODS are considerable—they account for 50% of annual mean Arctic surface warming and 58% of September sea-ice loss over the period 1955–2005.

How can ODS, which contribute only ~20% of the GHG RF over the Arctic over that period (see Methods), cause such a large forced surface warming and sea-ice loss? It has been reported[24] that ODS produce a larger global surface warming per unit RF than any other well-mixed GHG (larger than CO_2, CH_4 and N_2O)—in other words,

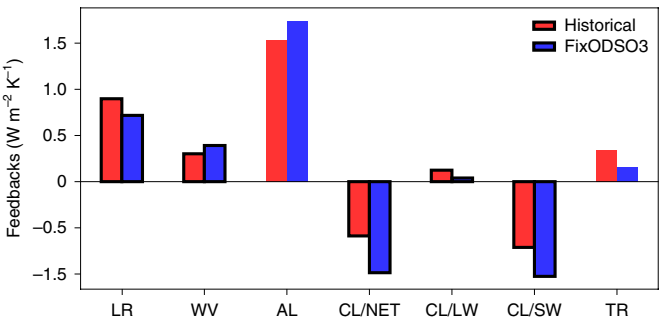

Fig. 4 | Arctic feedbacks for 1955–2005. Annual mean, ensemble mean Arctic feedbacks in the Historical (red) and FIXODSO3 (blue) integrations with CAM5LE (see Methods for details) for the lapse rate (LR), water vapour (WV), albedo (AL), cloud (CL/NET) and energy transport (TR) components. Cloud feedback is further subdivided into long-wave (CL/LW) and short-wave (CL/SW) components. Statistically significant feedbacks (those for which two-thirds or more of ensemble members are in agreement on the sign of the Historical minus FixODSO3 difference) are highlighted with black outlines.

that they have the highest warming 'efficacy'. However, that result from a single model has not been independently confirmed and the precise value of ODS efficacy remains to be robustly quantified. More broadly, the impact of ODS on Arctic surface warming has not been studied in detail. As a starting point towards understanding the high efficacy of ODS, we performed a standard feedback analysis[25] for the Arctic (see Methods and Fig. 4). In addition to a larger RF, two factors produce an enhanced Arctic warming with increasing ODS in CAM5LE: (1) a stronger lapse rate feedback (which is positive for the Arctic, confirming previous work[26]) and (2) a weaker negative net cloud feedback (with contributions from both long and short waves). The surface albedo feedback is not significantly different between the Historical and FixODSO3 ensembles. These findings are robust, because they are confirmed by a similar feedback analysis for the integrations with WACCM4 (see Extended Data Fig. 5), a climate model with very different physical parameterizations.

Beyond the specific physical mechanisms responsible for the high efficacy of ODS on the Arctic climate system, it is important to place ODS in the context of the other anthropogenic forcings. As seen in Fig. 1, the largest RF is associated with CO_2, and it is three times larger than the RF from ODS, over the 1955–2005 period. At the same time, anthropogenic aerosols are believed to have

produced a considerable, yet highly uncertain, negative[7] RF. Without the large cancellation from aerosols the relative contribution of ODS to the total forced Arctic climate change would be smaller. However, irrespective of aerosols, the absolute contribution of ODS—nearly 0.8 °C of warming and 0.7×10^6 km^2 of September sea ice loss over only 50 years—is remarkably large.

In conclusion, if our findings are confirmed by future studies, the role of the Montreal Protocol as a major environmental treaty will assume a new dimension. Our model integrations show that, in addition to being the key drivers of stratospheric ozone depletion (notably over the South Pole), ODS have been important players in the global climate system, notably in the Arctic, over the second half of the twentieth century. Our findings also have implications for the future because the phase-out of ODS, which is well under way, will substantially mitigate Arctic warming and sea-ice melting in the coming decades.

Online content

Any methods, additional references, Nature Research reporting summaries, source data, extended data, supplementary information, acknowledgements, peer review information; details of author contributions and competing interests; and statements of data and code availability are available at https://doi.org/10.1038/s41558-019-0677-4.

Received: 8 May 2019; Accepted: 3 December 2019;
Published online: 20 January 2020

References

1. Bindoff, N. L. et al. in *Climate Change 2013: The Physical Science Basis* (eds Stocker, T. F. et al.) 867–952 (IPCC, Cambridge Univ. Press, 2013).
2. Engel, A. et al. in *Scientific Assessment of Ozone Depletion: 2018* Report No. 58, Ch. 1 (Global Ozone Research and Monitoring Project, 2018).
3. Ramanathan, V. Greenhouse effect due to chlorofluorocarbons: climatic implications. *Science* **190**, 50–52 (1975).
4. Solomon, S. Stratospheric ozone depletion: a review of concepts and history. *Rev. Geophys.* **37**, 275–316 (1999).
5. Farman, J. C., Gardiner, B. G. & Shanklin, J. D. Large losses of total ozone in Antarctica reveal seasonal ClO_x/NO_x interaction. *Nature* **315**, 207–210 (1985).
6. World Meteorological Organization/United Nations Environmental Program *Scientific Assessment of Ozone Depletion: 2018* Report No. 58 (Global Ozone Research and Monitoring Project, 2018).
7. Myhre, G. et al. in *Climate Change 2013: The Physical Science Basis* (eds Stocker, T. F. et al.) Ch. 8 (IPCC, Cambridge Univ. Press, 2013).
8. Young, P. J. et al. Agreement in late twentieth century Southern Hemisphere stratospheric temperature trends in observations and CCMVal-2, CMIP3, and CMIP5 models. *J. Geophys. Res. Atmos.* **118**, 605–613 (2013).
9. Son, S.-W., Tandon, N. F., Polvani, L. M. & Waugh, D. W. Ozone hole and Southern Hemisphere climate change. *Geophys. Res. Lett.* **36**, L15705 (2009).
10. Kang, S., Polvani, L., Fyfe, J. & Sigmond, M. Impact of polar ozone depletion on subtropical precipitation. *Science* **332**, 951–954 (2011).
11. Thompson, D. W. et al. Signatures of the Antarctic ozone hole in Southern Hemisphere surface climate change. *Nat. Geosci.* **4**, 741–749 (2011).
12. Previdi, M. & Polvani, L. M. Climate system response to stratospheric ozone depletion and recovery. *Q. J. R. Meteorol. Soc.* **140**, 2401–2419 (2014).
13. Ramanathan, V. et al. Climate–chemical interactions and effects of changing atmospheric trace gases. *Rev. Geophys.* **25**, 1441–1482 (1987).
14. Shine, K. P. On the cause of the relative greenhouse strength of gases such as the halocarbons. *J. Atmos. Sci.* **48**, 1513–1518 (1991).
15. Hodnebrog, Ø. et al. Global warming potentials and radiative efficiencies of halocarbons and related compounds: a comprehensive review. *Rev. Geophys.* **51**, 300–378 (2013).
16. Meinshausen, M. et al. The RCP greenhouse gas concentrations and their extensions from 1765 to 2300. *Climatic Change* **109**, 213 (2011).
17. Forster, P. et al. in *Climate Change 2007: The Physical Science Basis* (eds Solomon, S. et al.) Ch. 2 (IPCC, Cambridge Univ. Press, 2007).
18. Velders, G. J., Andersen, S. O., Daniel, J. S., Fahey, D. W. & McFarland, M. The importance of the Montreal Protocol in protecting climate. *Proc. Natl Acad. Sci. USA* **104**, 4814–4819 (2007).
19. Estrada, F., Perron, P. & Martínez-López, B. Statistically derived contributions of diverse human influences to twentieth-century temperature changes. *Nat. Geosci.* **6**, 1050–1055 (2013).
20. Overland, J., Walsh, J. & Kattsov, V. in *Snow, Water, Ice and Permafrost in the Arctic (SWIPA) 2017* 9–24 (Arctic Monitoring and Assessment Programme, 2017).
21. Vaughan, D. et al. in *Climate Change 2013: The Physical Science Basis* (eds Stocker, T. F. et al.) Ch. 4 (IPCC, Cambridge Univ. Press, 2013).
22. Kay, J. et al. The Community Earth System Model (CESM) large ensemble project: a community resource for studying climate change in the presence of internal climate variability. *Bull. Am. Meteorol. Soc.* **96**, 1333–1349 (2015).
23. Deser, C., Phillips, A., Bourdette, V. & Teng, H. Uncertainty in climate change projections: the role of internal variability. *Clim. Dynam.* **38**, 527–546 (2012).
24. Hansen, J. E. et al. Efficacy of climate forcings. *J. Geophys. Res. Atmos.* **110**, D18104 (2005).
25. Soden, B. J. et al. Quantifying climate feedbacks using radiative kernels. *J. Clim.* **21**, 3504–3520 (2008).
26. Pithan, F. & Mauritsen, T. Arctic amplification dominated by temperature feedbacks in contemporary climate models. *Nat. Geosci.* **7**, 181–184 (2014).
27. Hansen, J., Ruedy, R., Sato, M. & Lo, K. Global surface temperature change. *Rev. Geophys.* **48**, RG4004 (2010).
28. Titchner, H. A. & Rayner, N. A. The Met Office Hadley Centre sea ice and sea surface temperature data set, version 2: 1. sea ice concentrations. *J. Geophys. Res. Atmos.* **119**, 2864–2889 (2014).

Methods

ODS. ODS are organic chlorine and bromine compounds regulated by the Montreal Protocol, and include CFCs, hydrochlorofluorocarbons (HCFCs), halons, carbon tetrachloride, methyl chloride, methyl chloroform and several others. In CAM5LE only two ODS are prescribed, CFC-11. and CFC-12: their time-dependent concentrations are identical at all latitudes, longitudes and heights in the atmosphere. CFC-11. is a linear combination of CFC-11 and several other halocarbons (CF_4, C_2F_6, C_6F_{14}, HFC-23, HFC-32, HFC43_10, HFC-125, HFC-134a, HFC-143a, HFC-227ea, HFC-245fa, SF_6, CFC-113, CFC-114, CFC-115, CCl_4, CH_3CCl_3, HCFC-22, HCFC-141B, HCFC-142B, Halon-1211, Halon-1301, Halon-2402, CH_3Br and CH_3Cl), prorated by their radiative efficiency relative to CFC-11. In WACCM4 the following ODS are included: CFC-11, CFC-12, CFC-113, CFC-114, CFC-115, HCFC-22, HCFC-141b, HCFC-142b, Halon-1211, Halon-1301, Halon-1202, Halon-2402, CCl_4, CH_3Cl, CH_3CCl_3, CH_3Br, CH_2Br_2 and $CHBr_3$. In that model, their surface concentrations are specified and these species are then advected into the atmosphere and undergo chemical reactions. However, only some of these are radiatively active—specifically, CFC-11, CFC-113, CCl_4, CH_3CCl_3, HCFC-22, Halon-1211 and Halon-1301 are combined into CFC-11. which, together with CFC-12, is passed to the radiative transfer module.

Models. Three models are used for this study, all part of the Community Earth System Model (CESM) Project. The first, denoted CAM5LE, is the low-top version of the Community Atmospheric Model, Version 5, coupled to land, ocean and sea-ice components as configured for the Large Ensemble Project[22]. In CAM5LE both ozone and ODS are prescribed from input files. The trends and variability of Arctic sea ice in CAM5LE are extensively documented in the literature[29,30] and compare very well[31] with observations.

The second, denoted WACCM4, is the top member of CESM with interactive chemistry for stratospheric ozone[32], and is also coupled to land, ocean and sea-ice components. Only the surface concentrations of ODS are prescribed, since ozone is computed. The physical parameterizations in WACCM4 are very different from those in CAM5LE, and these differences have been shown to substantially affect climate sensitivity[33]. It is, therefore, a distinct climate model.

The third, denoted PORT, is the offline radiative component[34] of CESM. We used it to compute radiative forcing (ΔR_F) associated with specific atmospheric composition changes. We compute ΔR_F with stratospheric adjustment under the assumption[7,34] of fixed dynamical heating.

Model integrations. For the Historical integrations, both CAM5LE and WACCM4 are forced with all known natural and anthropogenic forcings, as specified by the Coupled Model Intercomparison Project[35], Phase 5 (CMIP5). The CAM5LE Historical integrations analysed here are provided by CESM Large Ensemble Project[22] for the period 1955–2005. The WACCM4 Historical integrations analysed here are the contribution[32] of the CESM Whole Atmosphere Community Climate Model Working Group to CMIP5. For both of these models, the simulated climate over the historical period has been carefully documented. For the FixODSO3 integrations, we force the models as follows: for CAM5LE, both CFCs and stratospheric ozone were held constant at 1955 values, but for WACCM4 only ODS were held constant and stratospheric ozone remained approximately constant as a consequence (but is computed by the model, consistently with the atmospheric circulation). For the FixODS integrations in CAM5LE, only ODS were held constant and ozone depletion was prescribed as in the Historical integrations. Note that FixODS integrations cannot be performed with WACCM4, because ozone depletion cannot take place with constant ODS. We emphasize that, for the FixODSO3 and FixODS integrations, we ran the identical model code as the corresponding Historical integrations (for both CAM5LE and WACCM4): only the forcing files were changed.

For CAM5LE we analyse ten integrations for each of the three ensembles (Historical, FixODSO3 and FixODS). With WACCM4, we analyse six integrations each with Historical and FixODSO3 forcings. In each case, the forced response is defined as the ensemble mean 'change' (see the following subsection).

Analysis. For any variable of interest, we define 'change' as the difference between the last and first decades of the model integrations—that is, the mean of years 1996–2005 minus the mean of years 1955–1964. From this, we compute 'trend' as the change divided by the number of years (51). This procedure is preferred to a simple linear trend, as the ODS and ozone time-series are more similar to sigmoid functions than to straight lines.

Feedback analysis. The annual mean energy budget at the top-of-atmosphere (TOA) for the Arctic climate system (60–90° N, area weighted) can be written in the form

$$R + F = H \tag{1}$$

where R is the net downward radiation at the TOA, F is the horizontal convergence of the atmospheric and oceanic energy fluxes and H is the net heat uptake by the Arctic climate system. All quantities are in units of W m^{-2}. Neglecting the heat capacity of the atmosphere, heat uptake by the land surface and the melting of perennial snow and ice cover, H is then approximated by the ocean heat uptake, denoted H_o.

Next, we focus on the change in this energy budget between the first and last decades of the model integrations (1996–2005 minus 1955–1964), expressed by the symbol Δ, so that

$$\Delta R + \Delta F - \Delta H_o = 0 \tag{2}$$

As is customary, the change ΔR in TOA radiation is decomposed into ΔR_F due to changes in the atmospheric composition, and additional radiative contributions from surface and tropospheric temperatures (ΔR_T), tropospheric water vapour (ΔR_{WV}), surface albedo (ΔR_{AL}) and clouds ($\Delta R_{CL/NET}$), with the last of these being further decomposed into long- and short-wave components, $\Delta R_{CL/LW}$ and $\Delta R_{CL/SW}$, respectively. This yields

$$\Delta R = \Delta R_F + \Delta R_T + \Delta R_{WV} + \Delta R_{AL} + \Delta R_{CL/LW} + \Delta R_{CL/SW} \tag{3}$$

We compute ΔR_F with the PORT model[34], including the rapid stratospheric temperature adjustment. For the Historical integrations, ΔR_F includes well-mixed GHGs (including ODS) and ozone (both tropospheric and stratospheric). For the FixODSO3 integrations, ΔR_F includes only the effects of changes in the non-ODS well-mixed GHGs (CO_2, CH_4 and N_2O) and tropospheric ozone; for the FixODS integrations, stratospheric ozone is also included. For the Arctic mean, we find $\Delta R_F = 1.26$, 1.01 and 1.10 W m^{-2} for the Historical, FixODSO3 and FixODS cases, respectively.

All other terms in equation (3) are computed using the radiative kernel[25] method. For $\Delta R_{CL/NET}$, $\Delta R_{CL/LW}$ and $\Delta R_{CL/SW}$ we adjust the model output cloud radiative forcing (CRF) change to account for changes in non-cloud variables[25,36,37]. All terms in equation (3) are area-averaged over the Arctic (60–90° N). ΔR_T and ΔR_{WV} are vertically integrated from the surface to the tropopause.

The radiative changes associated with temperature changes are further decomposed into a Planck response (ΔR_{Planck}) and a lapse rate feedback (ΔR_{LR}),

$$\Delta R_T = \Delta R_{Planck} + \Delta R_{LR} \tag{4}$$

By construction, ΔR_{Planck} represents TOA radiation change resulting from a vertically uniform warming of magnitude ΔT_s, while ΔR_{LR} represents the additional TOA radiation change due to vertically non-uniform warming. The Planck response, then, is directly proportional to the change in Arctic mean surface temperature, given as

$$\Delta R_{Planck} = \lambda_0 \, \Delta T_s \tag{5}$$

where λ_0 is the proportionality constant. In the absence of feedbacks, $1/\lambda_0$ can be thought of as the Arctic climate sensitivity parameter[38]. From our radiative kernels[39] we find $\lambda_0 = -2.61$ W m^{-2} K^{-1} for the Arctic mean, which is slightly lower than the global mean value of −3.1 W m^{-2}K^{-1}.

The other feedbacks are obtained by substituting equation (4) into equation (3) and writing the remaining terms in the form $\Delta R_X = \lambda_X \Delta T_s$, for the variable X=LR, WV, AL, CL/NET, CL/SW and CL/LW. The values of the 'feedback parameters' λ_X, computed by dividing ΔR_X derived from the kernels by the corresponding surface warming, ΔT_s, in each model integration, are plotted in Fig. 4 and Extended Data Fig. 5, in units of W m^{-2} K^{-1}.

Finally, to close the energy budget, we need to estimate ΔF (see equation (2)). For consistency this is done as a residual, after separately computing ΔR and ΔH_o from model output. The rightmost item in Fig. 4 and Extended Data Fig. 5 shows $\lambda_{TR} \equiv \Delta F/\Delta T_s$, and represents the change in atmosphere and ocean energy transport into the Arctic caused by the forcings applied over the period of interest (1955–2005).

Data availability

All model output analysed in the study is currently stored on data servers at the National Center for Atmospheric Research in Boulder, CO, USA, and are available from the corresponding author on request. The GISTEMP[27] data are available at https://data.giss.nasa.gov/gistemp and the HadISST[28] data can be found at https://www.metoffice.gov.uk/hadobs/hadisst2.

Code availability

All code used to produce the figures are available from the corresponding author on request.

References

29. Jahn, A., Kay, J. E., Holland, M. M. & Hall, D. M. How predictable is the timing of a summer ice-free Arctic? *Geophys. Res. Lett.* **43**, 9113–9120 (2016).
30. Labe, Z., Magnusdottir, G. & Stern, H. Variability of Arctic sea ice thickness using PIOMAS and the CESM large ensemble. *J. Clim.* **31**, 3233–3247 (2018).
31. England, M. R., Jahn, A. & Polvani, L. M. Nonuniform contribution of internal variability to recent Arctic sea ice loss. *J. Clim.* **32**, 4039–4053 (2019).

32. Marsh, D. R. et al. Climate change from 1850 to 2005 simulated in CESM1 (WACCM). *J. Clim.* **26**, 7372–7391 (2013).
33. Gettelman, A., Kay, J. & Shell, K. The evolution of climate sensitivity and climate feedbacks in the community atmosphere model. *J. Clim.* **25**, 1453–1469 (2012).
34. Conley, A., Lamarque, J.-F., Vitt, F., Collins, W. & Kiehl, J. Port, a CESM tool for the diagnosis of radiative forcing. *Geosci. Model Dev.* **6**, 469–476 (2013).
35. Taylor, K. E., Stouffer, R. J. & Meehl, G. A. An overview of CMIP5 and the experiment design. *Bull. Am. Meteorol. Soc.* **93**, 485–498 (2012).
36. Previdi, M. Radiative feedbacks on global precipitation. *Environ. Res. Lett.* **5**, 025211 (2010).
37. Previdi, M. & Liepert, B. G. The vertical distribution of climate forcings and feedbacks from the surface to top of atmosphere. *Clim. Dynam.* **39**, 941–951 (2012).
38. Roe, G. Feedbacks, timescales, and seeing red. *Annu. Rev. Earth Planet. Sci.* **37**, 93–115 (2009).
39. Pendergrass, A. G., Conley, A. & Vitt, F. M. Surface and top-of-atmosphere radiative feedback kernels for CESM-CAM5. *Earth Syst. Sci. Data* **10**, 317–324 (2018).

Acknowledgements

All computations were performed with resources provided by the Computational and Information Systems Laboratory at the National Center for Atmospheric Research, which is sponsored by the US National Science Foundation. The historical CAM5LE integrations were performed by the Large Ensemble[22] Project. This research was funded by two grants from the USNSF to Columbia University. L.M.P. is grateful to J. Kay, and the other organizers, for the opportunity to attend the 2018 CESM Polar Modeling Workshop in Boulder, CO, USA. The authors are indebted to P. Forster and J. Fyfe for suggesting an important clarification.

Author contributions

L.M.P. designed the study, carried out WACCM4 integrations and wrote the first draft of the manuscript. M.P. suggested and performed feedback analysis. M.R.E. carried out CAM5LE integrations and helped with their analysis. G.C. computed radiative forcing with the PORT model. K.L.S. helped with analysis of WACCM4 integrations. All authors contributed to the interpretation of the results and to the drafting of the final manuscript.

Competing interests

The authors declare no competing interests.

Additional information

Extended data is available for this paper at https://doi.org/10.1038/s41558-019-0677-4.

Correspondence and requests for materials should be addressed to L.M.P.

Peer review information *Nature Climate Change* thanks Francisco Estrada and the other, anonymous, reviewer(s) for their contribution to the peer review of this work.

Reprints and permissions information is available at www.nature.com/reprints.

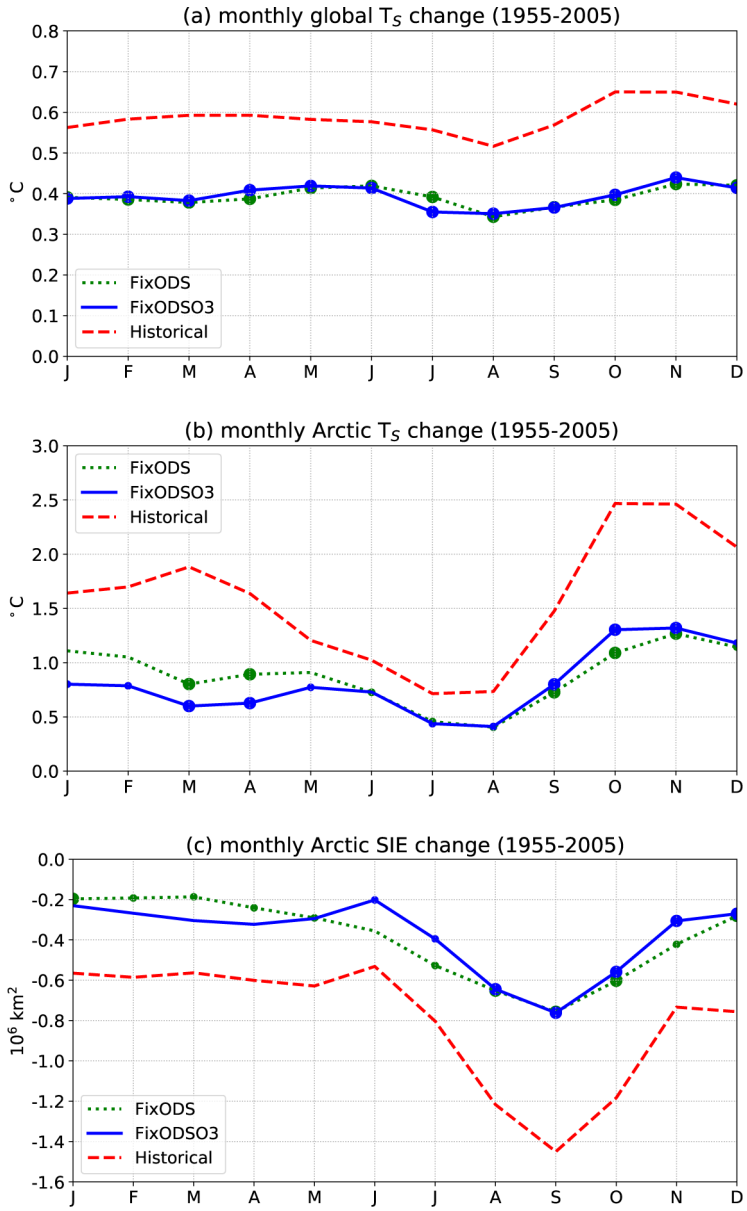

Extended Data Fig. 1 | Seasonal changes, 1955-2005. Monthly, ensemble-mean, 1955-2005 change in (a) global and (b) Arctic surface air temperature (T_s) and (c) Sea Ice Extent (SIE, the total area with sea ice concentration exceeding 15%), in the CAM5LE model. On the curves for the FixODSO3 and FixODS ensembles, small and large circles highlight the months in which the difference with the Historical ensemble is statistically significant at the 95% and 99% level, respectively, (from a two-tailed t-test).

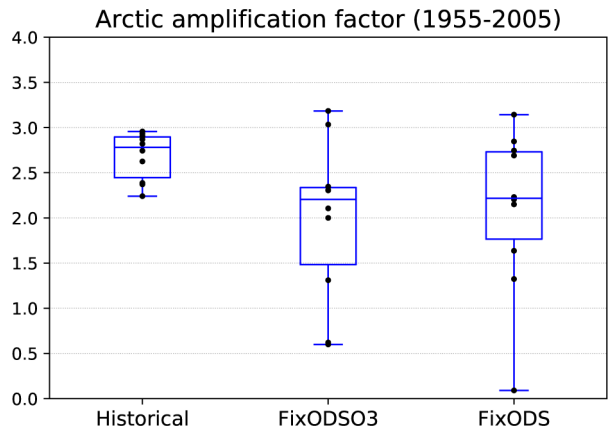

Extended Data Fig. 2 | Arctic amplification, 1955-2005. Arctic amplification factor for the three CAM5LE ensembles over the period 1955-2005. The factor is defined as the annual mean surface air temperature change over the Arctic (60-90˚N) divided by the corresponding global mean change. The boxes extend from the lower to upper quartile, with a line at the median, and with whiskers showing the entire range across each ensemble; the individual members are shown by the small black dots. The difference between the means of the FixODSO3 and Historical ensembles is statistically significant at the 95% level.

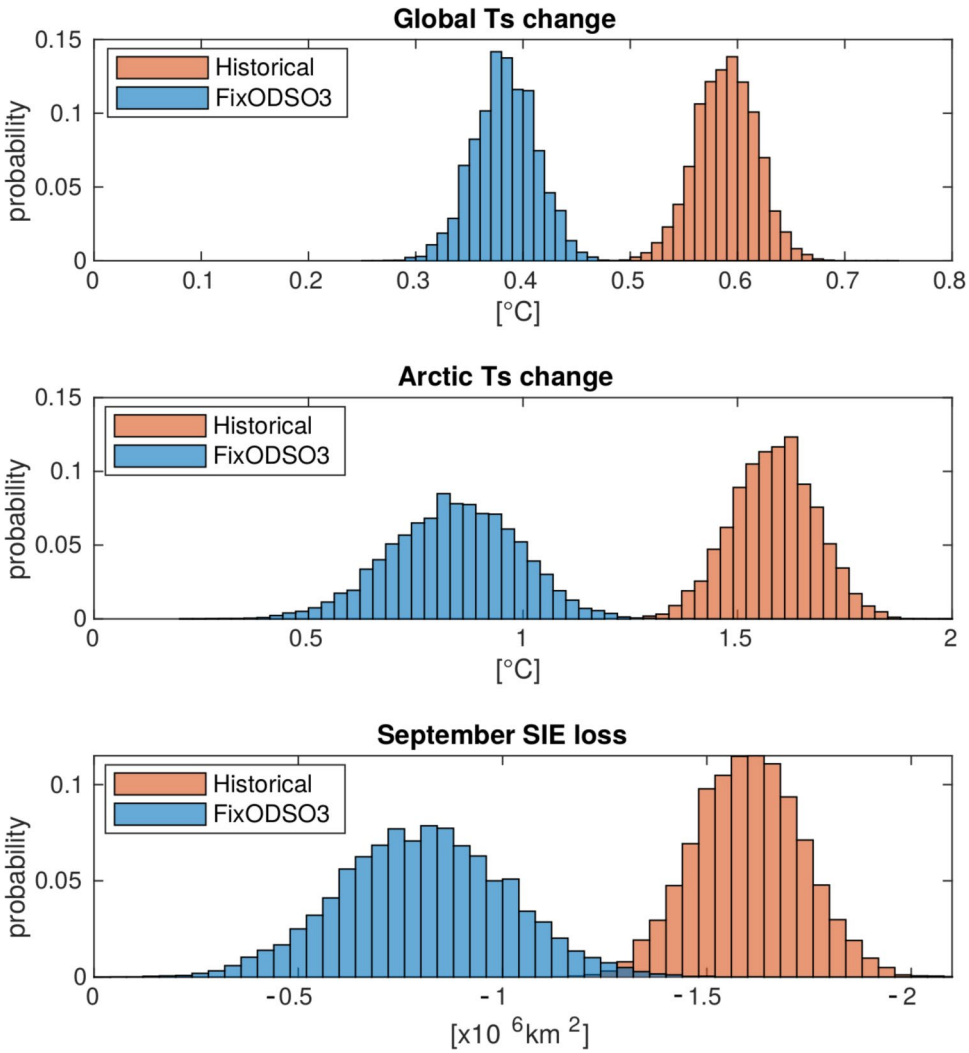

Extended Data Fig. 3 | Synthetic PDFs of 1955-2005 changes. Probability distribution functions (PDFs) of annual global surface temperature change (top), Arctic surface temperature change (middle), and September sea ice loss computed from the Historical (red) and FixODSO3 (blue) simulations with the CAM5LE model. These PDFs are constructed by 'resampling with replacement' âĂŞ 10,000 times âĂŞ the original set of 10 model simulations.

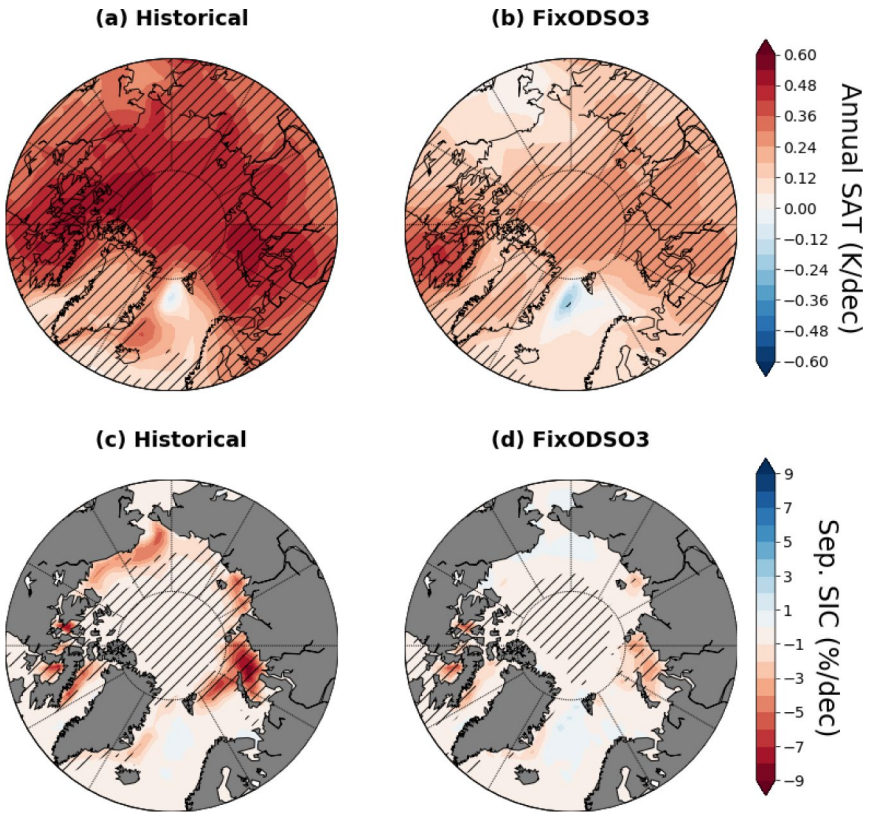

Extended Data Fig. 4 | Arctic surface temperature and sea ice trends, 1955-2005. As in Fig. 2, but for the WACCM4 model integrations.

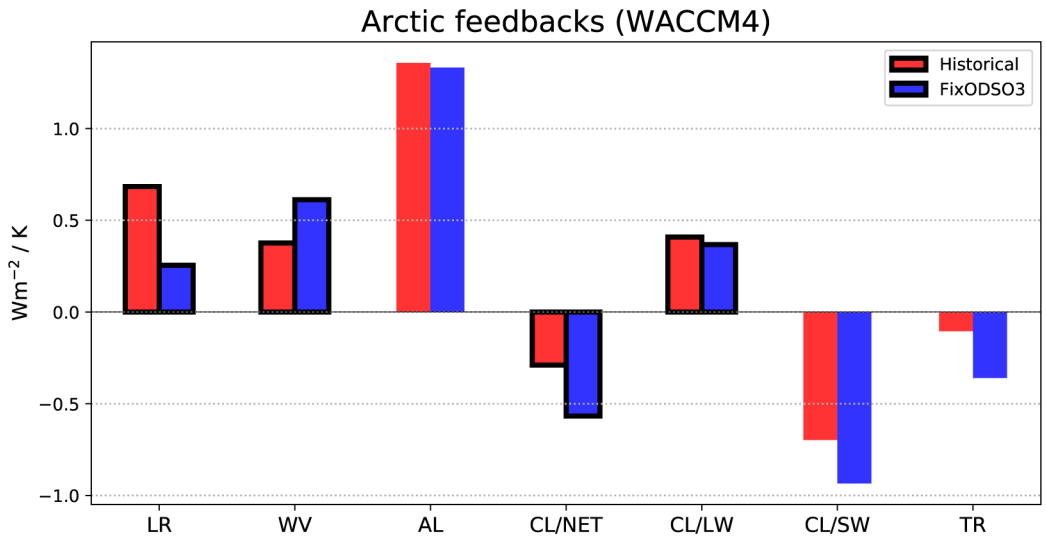

Extended Data Fig. 5 | Arctic feedbacks, 1955-2005. As in Fig. 4, but for the WACCM4 model integrations.